

## ZEOLITES, PREHNITE, AND PUMPELLYITE FROM BERTRIX, BELGIAN ARDENNES

Frédéric HATERT<sup>1</sup> & Thomas THEYE<sup>2</sup>

<sup>1</sup> *Laboratoire de Minéralogie, Université de Liège, B.18, B-4000 Liège, Belgium*

<sup>2</sup> *Institut für Mineralogie und Kristallchemie, Universität Stuttgart, Azenbergstrasse 18, D-70174 Stuttgart, Germany*

(10 figures, 2 tables)

**Abstract.** Laumontite, stilbite-Ca, chabazite-Ca, natrolite and/or tetranatrolite, prehnite, and pumpellyite-(Fe<sup>2+</sup>) were observed in fractures crosscutting the amphibolite-facies metamorphic rocks from Bertrix, Belgian Ardennes. The minerals are characterised by their unit-cell parameters and chemical analyses. The infrared spectra of stilbite and chabazite are also discussed. The P-T conditions of formation of laumontite are  $2 \pm 1$  kbar / 200-250°C, in good agreement with the maximum stability ranges of prehnite and pumpellyite. This P-T range could represent an extensional event on a smooth retrograde cooling path.

**Keywords:** zeolites, prehnite, pumpellyite, low-grade metamorphism.

**Résumé.** Laumontite, stilbite-Ca, chabazite-Ca, natrolite et/ou tétranatrolite, prehnite et pumpellyite-(Fe<sup>2+</sup>) ont été identifiées dans les fractures recoupant les roches métamorphiques de Bertrix, Ardennes belges. Ces minéraux sont caractérisés par leurs paramètres cristallographiques et par leurs analyses chimiques. Les spectres infrarouges de la stilbite et de la chabazite sont également discutés. Les conditions de formation de la laumontite,  $2 \pm 1$  kbar / 200-250°C, sont en accord avec les domaines de stabilité de la prehnite et de la pumpellyite. Ces conditions P-T pourraient représenter un épisode d'extension au cours d'une phase métamorphique rétrograde.

**Mots-clés:** zéolites, prehnite, pumpellyite, métamorphisme de faible degré, Bertrix, Ardennes belges.

### 1. Introduction

Laumontite was the first zeolite mineral described in the metamorphic zone of Libramont, Belgian Ardennes (Antun, 1953). Recently, the discovery of three new occurrences of this mineral around Bertrix initiated a detailed mineralogical study of laumontite from this area (Hatert, 1998). The significance of other zeolites and Ca-aluminosilicates associated with laumontite is reported in this note.

Zeolite minerals, prehnite, and pumpellyite samples have been collected in the quarry "Carrière de la Flèche", 3 km northwest of Bertrix. These minerals occur in the fractures crosscutting quartzites and schists of Lochkovian sedimentation age, affected by the Hercynian metamorphism. The paragenesis of the rocks from the Bastogne area, containing andalusite, plagioclase, biotite, hornblende, garnet and magnetite, is characteristic of low P-medium T conditions estimated around 2 kbar / 400°C (Beugnies, 1986). Data obtained by Theye & Fransolet (1993) on assemblages containing garnet, plagioclase, and hornblende indicate P-T conditions up to 3-4 kbar / 500°C in the area of Libramont. The formation of zeolites crosscutting the metamorphic rocks is related to the retrograde metamorphic evolution. Laumontite crystallised at the expense of plagioclase, under a pressure lower than 3 kbar and between 280 and 170°C, as estimated by Hatert (1998).

The aim of this paper is to present new mineralogical data on the zeolites and Ca-aluminosilicates from the quarry "Carrière de la Flèche" at Bertrix, and to discuss their significance. The occurrence of these minerals also constrains the P-T path followed during retrograde metamorphism.

### 2. Experimental

Identification of the minerals was performed with a Debye-Scherrer camera (diameter 114.6 mm) or a diffractometer equipped with a graphite monochromator (FeK<sub>α</sub> radiation,  $\lambda = 1.9373$  Å). The unit cell parameters were calculated with the least-squares refinement program LCLSQ 8.4 (Burnham, 1991), from the d-spacings corrected with an internal standard of Pb(NO<sub>3</sub>)<sub>2</sub>. Single-crystal measurements were performed with a Weissenberg goniometer using CuK<sub>α</sub> radiation ( $\lambda = 1.5418$  Å).

Wet chemical analyses were performed on 70 to 85 mg of material carefully selected under the binocular lens and checked for purity by X-ray diffraction. Atomic absorption spectrophotometry served to determine Si, Al, Fe, Mg, Ca, Sr, Na and K. The amount of H<sub>2</sub>O was measured by weight loss through heating of the mineral at 1050°C during two hours.

Electron microprobe analyses (EMPA) were performed at Louvain-la-Neuve with a CAMECA SX50 instrument, under an accelerating voltage of 15 kV and a probe current of 20 nA. A beam size of 2.5  $\mu\text{m}$  was used for prehnite and pumpellyite, and of 10 to 20  $\mu\text{m}$  for the zeolites, in order to avoid loss of water caused by beam damage. The standards used were oligoclase (Na), olivine (Mg), leucite (K), wollastonite (Ca, Si), barite (Ba), hematite (Fe), rhodonite (Mn), corundum (Al), and strontianite (Sr). Additional microprobe analyses were performed at Stuttgart University with a SX100 instrument, applying similar conditions and standards except for Mg (periclase), K (orthoclase) and Na (albite).

The infrared spectra of chabazite and stilbite were recorded on a Nicolet MAGNA-IR 760 spectrometer, from 50 scans with a 2  $\text{cm}^{-1}$  resolution, in the range 400–4000  $\text{cm}^{-1}$ . The samples were prepared by mixing intimately 0.3 mg of zeolite powder with KBr, in order to obtain a 150 mg homogeneous pellet, which was dried for few hours at 140°C. To prevent water contamination, the measurements were performed under a dry-air purge.

Scanning electron microscope photographs were taken with a JEOL JSM-5800 microscope, after coating of the sample with Au. Drawings of the crystals were realised with the SHAPE software (Dowty, 1994).

### 3. Petrography of the Bertrix rocks

The mineral assemblages, as observed in the millimetre-sized veins and in their country rocks with a binocular lens and with a polarising microscope, are compiled in Table 1, and their electron microprobe analyses are given in Table 2.

#### 3.1. Zeolites and pumpellyite-bearing veins

Laumontite-bearing fractures contain additional chlorite, calcite, and prehnite as accessory minerals. Laumontite appears intimately intergrown with chlorite in some cases. The stilbite-bearing fractures contain stilbite and/or chabazite. Stilbite grows on fissures of the country rock

without any signs of reaction textures. Even biotite that is sensitive to late alteration remains stable directly adjacent to the vein containing stilbite.

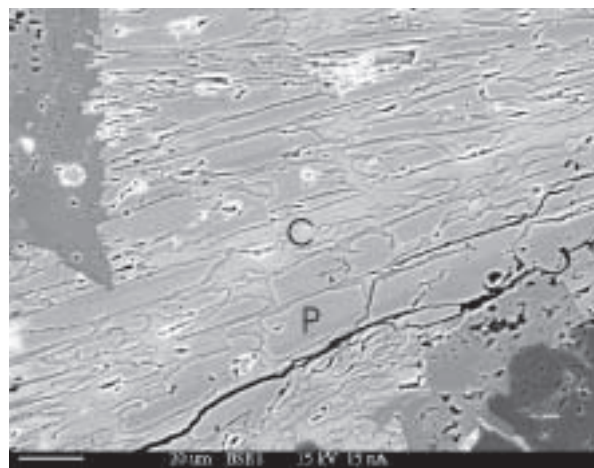


**Figure 1.** Scanning electron microscope image showing the replacement of pumpellyite (gray acicular relics, P) by calcite (light gray interstitial phase, C). Back-scattered electron image, sample Bert9.

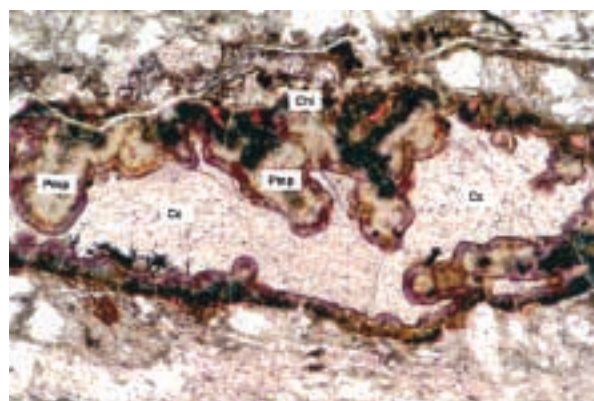


**Figure 2.** Association pumpellyite (Pmp) + calcite (Cc) + chlorite (Chl), occurring in the fractures from Bertrix. Transmitted light polarising microscope, 250  $\mu\text{m}$ .

Fracture type	Assemblage of the vein	Assemblage of the country rock
Laumontite	Laumontite-chlorite-calcite-prehnite	Quartz-muscovite-plagioclase-ilmenite-tourmaline-chlorite
Stilbite	Stilbite-chabazite	Quartz-muscovite-plagioclase-chlorite-biotite-ilmenite
Natrolite	Natrolite	Not observed
Pumpellyite	Pumpellyite-calcite-chlorite-K feldspar	Quartz-muscovite-plagioclase-chlorite-ilmenite-rutile-apatite-zircon-microcline-calcite-tourmaline-pumpellyite

**Table 1.** Mineral assemblages of the fractures and of their country rocks, Bertrix, Belgian Ardennes.

Under the polarising microscope, three generations of veins can be distinguished in the pumpellyite-bearing rocks. The earlier generation contains pumpellyite, and its formation is probably related to albitisation of plagioclase. Pumpellyite is also present in the country rock in the vicinity of the veins. The pumpellyite is partly replaced by calcite (Fig. 1). A second vein generation consists of a rim composed of K-feldspar, that contains numerous small inclusions of the country rock minerals. This rim was formed by a crack-seal mechanism. An inner portion of the vein contains coarser-grained K-feldspar and calcite. These minerals probably crystallised within open fissures. The formation of K-feldspar is related to the chloritisation of biotite, and calcite may have been formed at the expense of plagioclase and pumpellyite. The third vein formation in the pumpellyite-bearing rocks is constituted by very fine-grained brownish phyllosilicates associated with calcite. The three different vein generations are partly using the same channelways, and a rather complex pattern may result (Fig. 2). Besides the formation of vein minerals, there was also some removal of material by solution processes as indicated by a concentration of insoluble material such as opaque minerals along the vein boundaries.

### 3.2. Country rocks

The country rocks of the veins are constituted by weakly foliated metapelites, with mineral paragenesis of quartz, muscovite, plagioclase, chlorite and ilmenite. As accessory minerals, biotite and tourmaline are observed in the stilbite-bearing and laumontite-bearing rocks, respectively, whereas rutile, apatite, zircon, K-feldspar, calcite, and tourmaline occur in the pumpellyite-bearing rocks. The boundaries of the country rocks with the millimetre-sized veins are sharp.

## 4. Mineralogical description

### 4.1. Laumontite

Laumontite occurs as white to creamy white crystals with a pearly luster, forming radiated fibrous aggregates up to 4 cm in diameter. The wet chemical analysis from Hatert (1998) is reproduced in Table 2a (column 5), and compared with the electron microprobe analyses of the present study (columns 1 and 4). Both compositions are in good agreement with the structural formula of laumontite,  $\text{Ca}_4[\text{Al}_8\text{Si}_{16}\text{O}_{48}]\cdot 18\text{H}_2\text{O}$  (Coombs *et al.*, 1998). Crystallochemical data on laumontite from Bertrix and from other occurrences in this area (Lamouline, Luchy, Ochamps) have previously been discussed in detail by Hatert (1998).

wt % :	Lmt	Prh	Chl	Lmt	Lmt
No. :	Bert5	Bert5	Bert5	Bert1	Bert1
n :	7	12	5	9	*
SiO <sub>2</sub>	52.91	44.18	24.56	53.33	53.00
TiO <sub>2</sub>	0.02	-	0.06	-	-
Al <sub>2</sub> O <sub>3</sub>	22.20	24.63	22.79	21.64	21.27
MgO	0.28	-	13.62	-	0.04
FeO	0.61	0.01	24.94	0.03	0.15
MnO	0.02	0.01	0.56	-	-
CaO	11.61	27.90	0.17	12.10	10.89
SrO	-	0.05	-	0.08	0.03
BaO	0.02	-	0.02	-	-
Na <sub>2</sub> O	0.03	0.01	0.02	0.09	0.03
K <sub>2</sub> O	0.25	-	0.01	0.55	0.48
H <sub>2</sub> O	-	-	-	-	14.06
<b>Total</b>	<b>87.95</b>	<b>96.79</b>	<b>86.75</b>	<b>87.82</b>	<b>99.95</b>

Oxygen basis					
	48	11	14	48	48
Cation numbers					
Si	16.005	3.003	2.618	16.156	16.321
Ti	0.003	-	0.005	-	-
Al	7.917	1.973	2.863	7.727	7.720
Mg	0.125	-	2.163	-	0.018
Fe <sup>2+</sup>	0.154	0.001	2.223	0.008	0.039
Mn	0.006	-	0.051	-	-
<b>Sum</b>	<b>24.210</b>	<b>4.977</b>	<b>9.923</b>	<b>23.891</b>	<b>24.098</b>
Ca	3.763	2.031	0.019	3.928	3.593
Sr	-	0.002	-	0.014	0.005
Ba	0.003	-	0.001	-	-
Na	0.020	0.001	0.003	0.053	0.018
K	0.097	-	0.001	0.213	0.189
<b>Sum</b>	<b>3.883</b>	<b>2.034</b>	<b>0.024</b>	<b>4.208</b>	<b>3.805</b>
H	-	-	-	-	28.880

\* : Wet chemical analysis.

**Table 2.** Representative chemical analyses of minerals from Bertrix, Belgian Ardennes. Microprobe analyses, except otherwise indicated. Symbols for minerals are taken from Kretz (1983). Analysts : J.-M. Speetjens, T. Theye, and J. Wautier. **a.** Laumontite-bearing fractures.

#### 4.2. Stilbite-Ca

Micro-crystalline coatings occurring in stilbite-bearing fractures contain stilbite, sometimes associated with chabazite. The well-shaped crystals of stilbite, up to 1 mm long, show the forms  $\{010\}$ ,  $\{001\}$ ,  $\{110\}$  and  $\{11\bar{1}\}$ , with the less developed  $\{201\}$  faces (Figs 3 and 4). The parameters of the monoclinic unit cell were calculated in the  $C2/m$  setting:  $a = 13.638(3)$ ,  $b = 18.220(3)$ ,  $c = 11.270(2)$  Å, and  $\beta = 127.81(1)^\circ$ .

The chemical analyses (Table 2b, columns 1, 2 and 3) indicate a structural formula in good agreement with that proposed by Coombs *et al.* (1998),  $\square_{4.5}\text{Ca}_{4.5}[\text{Al}_9\text{Si}_{27}\text{O}_{72}]\cdot 28\text{H}_2\text{O}$ , for stilbite-Ca. Moreover, the substitution mechanisms  $\text{Si}^{4+} + \square \Rightarrow \text{Al}^{3+} + (\text{Na}^+, \text{K}^+)$  ( $\square$  denotes lattice vacancies) and  $\text{Ca}^{2+} \square + \Rightarrow \text{Na}^+ + \text{K}^+$  occur, responsible for the insertion of Na and K into the structure. These mechanisms are confirmed by the microprobe analyses (Table 2b, column 1), which indicate an excess of 0.182 Al on the tetrahedral sites, balanced by an excess of 0.210 charges on the large cation sites.

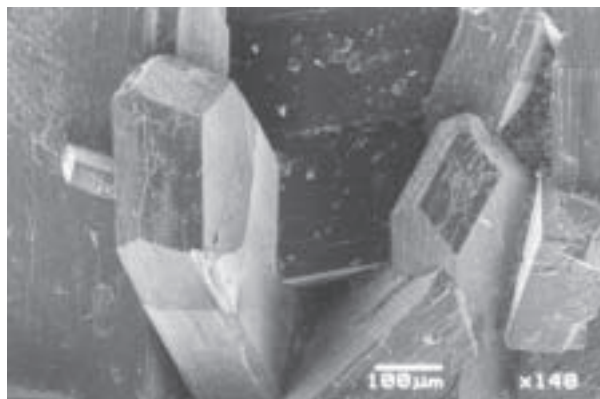


**Figure 3.** Stilbite from Bertrix, Belgium. A twinned crystal of chabazite can also be observed on the right side of the photograph. Secondary electron image.

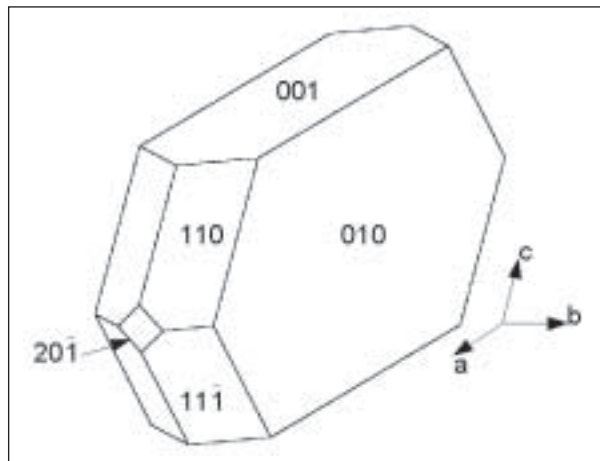


**Figure 4.** Morphology of stilbite from Bertrix.

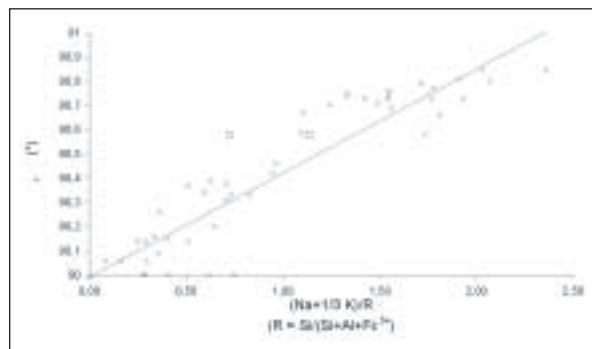


**Figure 5.** Relation between  $\beta$  and  $(\text{Na}+1/3 \text{ K})/\text{R}$  for stilbite and stellerite ( $\times$  = Passaglia *et al.*, 1978;  $\Delta$  = Ghobarkar *et al.*, 1999;  $\square$  = stilbite from Bertrix).

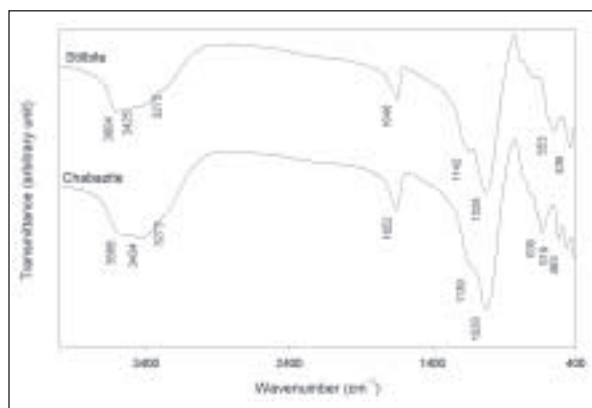


**Figure 6.** Infrared spectra of stilbite and chabazite from Bertrix.

Passaglia *et al.* (1978) explored the crystal chemistry of stilbite and stellerite, the Na-free orthorhombic equivalent of stilbite. These authors demonstrated that the incorporation of Na and K in the framework of stellerite implies an increase of the  $\beta$  angle from  $90^\circ$  to a maximum value of  $91^\circ$  for monoclinic stilbite ( $F2/m$  setting). Fig. 5 shows the variation of the  $\beta$  parameter versus the  $(\text{Na}+1/3 \text{ K})/\text{R}$  ratio ( $\text{R} = \text{Si}/(\text{Si}+\text{Al}+\text{Fe}^{3+})$ ), for natural stilbites and stellerites (Passaglia *et al.*, 1978), and for two synthetic samples (Ghobarkar *et al.*, 1999). Stilbite from Bertrix is in very good agreement with this diagram, thus confirming the coherence between the crystallographic and the chemical data presented for this sample.

The infrared spectrum of stilbite from Bertrix is characterised by the vibrations of the  $[(\text{Si},\text{Al})\text{O}_4]$  tetrahedra ( $400\text{--}1200 \text{ cm}^{-1}$ ) and of zeolitic water ( $1600\text{--}3700 \text{ cm}^{-1}$ ) (Fig. 6). The antisymmetric stretching and external vibrations of the  $[(\text{Si},\text{Al})\text{O}_4]$  tetrahedra, between  $900$  and  $1200 \text{ cm}^{-1}$  (Pechar & Rykl, 1985), show very broad absorption bands.

The absorption bands at  $3604$ ,  $3425$ , and  $3275 \text{ cm}^{-1}$  are characteristic of hydrogen bonds between  $\text{H}_2\text{O}$  and the crystal lattice. Starting from these absorption bands, calculations of  $\text{O}\dots\text{O}$  distances were performed using the

empirical relation proposed by Libowitzky (1999). The estimated O...O distances ( $\geq 3.00, 2.82,$  and  $2.73 \text{ \AA}$ ) are in agreement with those determined by Quartieri & Vezzalini (1987) for five stilbite samples ( $3.04$  to  $2.83 \text{ \AA}$ ).

#### 4.3. Chabazite-Ca

Frequently associated with stilbite, chabazite crystallizes as rhombohedral crystals up to 1 mm in length, showing the form  $\{10\bar{1}1\}$  with the less-developed  $\{02\bar{2}1\}$  and  $\{01\bar{1}2\}$  faces (Figs 7 and 8a). Rotation twins along  $[0001]$  have also been observed (Figs 7 and 8b). The parameters of the rhombohedral unit cell of chabazite from Bertrix were calculated in hexagonal setting:  $a = 13.790(3)$  and  $c = 15.011(6) \text{ \AA}$ .

The chemical analyses (Table 2b, columns 4 and 5) lead to a structural formula close to that suggested by Coombs *et al.* (1998),  $\square_2\text{Ca}_2[\text{Al}_4\text{Si}_8\text{O}_{24}]\cdot 12\text{H}_2\text{O}$ , for chabazite-Ca. It is interesting to note a relatively high Sr-content, as well as a replacement of Al by Si indicated by the Al/Si ratio lower than 0.5 (0.39 and 0.41). In order to obtain a stoichiometric formula, it is necessary to replace  $\text{Ca}^{2+}$  by  $(\text{K}^+, \text{Na}^+)$ , according to the substitution mechanism  $\text{Al}^{3+} + \text{Ca}^{2+} \Rightarrow \text{Si}^{4+} + (\text{K}^+, \text{Na}^+)$ . This mechanism is similar to that observed by Hatert (1998) for laumontite from Bertrix.

The crystal chemistry of chabazite was investigated by Passaglia (1970) who established a relation between the  $\text{Si}/(\text{Si}+\text{Al}+\text{Fe}^{3+})$  ratio and the  $c$  parameter. Chabazite samples from Bertrix are in very good agreement with the diagram proposed by this author (Fig. 9).

The infrared spectrum of chabazite from Bertrix is similar to that of stilbite from the same locality (Fig. 6), and the vibrations can be assigned according to Pechar & Rykl (1983). The O...O distances, calculated from the absorption bands related to the stretching vibrations of  $\text{H}_2\text{O}$  ( $3.07, 2.82,$  and  $2.73 \text{ \AA}$ ), are very close to those measured by Calligaris *et al.* (1982) on natural chabazite ( $3.13$  and  $2.81 \text{ \AA}$ ).

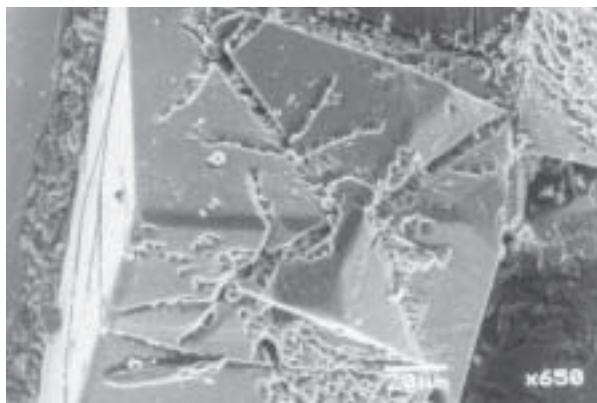


**Figure 7.** Rhombohedral crystals of chabazite from Bertrix, Belgium, showing the rotation twin along  $[0001]$ . Secondary electron image.

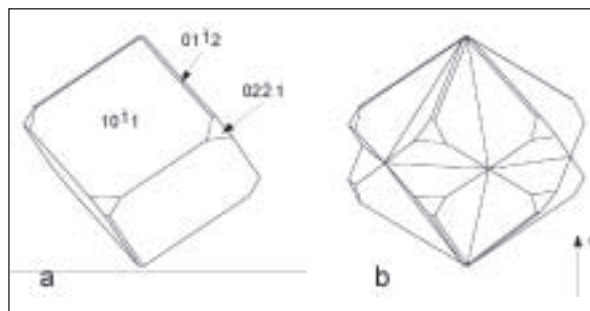


**Figure 8.** a. Morphology of chabazite from Bertrix. b. Rotation twin along  $[0001]$ .

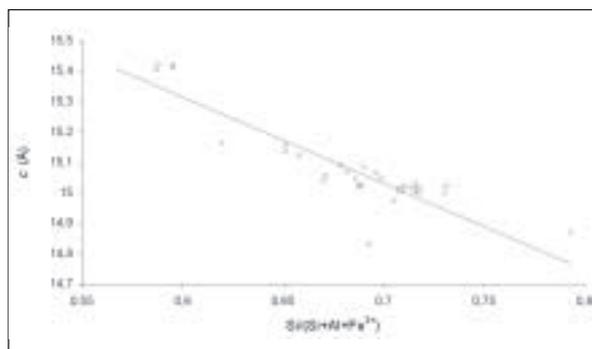


**Figure 9.** Relation between  $c$  and  $\text{Si}/(\text{Si}+\text{Al}+\text{Fe}^{3+})$  for chabazite ( $\times$  = Passaglia, 1970;  $\square$  = chabazite from Bertrix).

#### 4.4. Natrolite, tetranatrolite

A mineral of the natrolite mineral group forms a radiated fibrous aggregate of 1 cm diameter, constituted by white acicular crystals, covering the surface of a small sample. The microprobe analysis (Table 2b, column 6) leads to a structural formula corresponding to that of natrolite,  $\text{Na}_2[\text{Al}_2\text{Si}_3\text{O}_{10}]\cdot 2\text{H}_2\text{O}$  (Coombs *et al.*, 1998), but the substitution mechanism  $\text{Na}^+ + \text{Na}^+ \Rightarrow \text{Ca}^{2+} + \square$  occurs, indicated by the  $(\text{Na}^+ + \text{Ca}^{2+})$  sum of 1.80, lower than the ideal value of 2. The occurrence of small amounts of Ca, up to 0.11 atoms per formula unit, also indicates that this mineral could correspond to tetranatrolite,  $(\text{Na}, \text{Ca})_{16}[\text{Al}_9\text{Si}_{21}\text{O}_{80}]\cdot 16\text{H}_2\text{O}$ , because natrolite does not contain this element in significant amounts (Ross *et al.*, 1992).

The X-ray powder diffraction pattern is in very good agreement with that of tetranatrolite, but the single-crystal Weissenberg photograph shows that the analysed sample is probably constituted by a composite natrolite-tetranatrolite crystal, resulting from the epitactic overgrowth of tetranatrolite on natrolite (Chen & Chao, 1980). Despite the diffuse and elongate single-crystal X-ray reflections of tetranatrolite, the unit cell parameters of this tetragonal mineral were calculated:  $a = 13.15(9)$  and  $c = 6.610(7) \text{ \AA}$ . The observed reflections, with  $h + k + l = 2n$ , confirm the I-centred lattice of tetranatrolite.

wt % :	Stb	Stb	Stb	Cbz	Cbz	Ntr
No. :	Bert2	Bert2	Bert6	Bert3	Bert3	Bert4
n :	12	*	11	14	*	14
SiO <sub>2</sub>	59.93	56.34	60.33	52.01	50.17	47.45
TiO <sub>2</sub>	-	-	0.01	-	-	-
Al <sub>2</sub> O <sub>3</sub>	17.42	16.31	17.74	18.17	16.63	26.52
MgO	-	0.13	-	0.05	0.17	-
FeO	-	0.31	0.02	0.01	0.23	0.05
MnO	-	-	0.01	-	-	-
CaO	8.64	7.02	8.69	8.26	6.54	1.56
SrO	0.06	0.03	-	2.07	1.50	0.03
BaO	-	-	0.02	-	-	-
Na <sub>2</sub> O	0.42	0.72	0.28	0.21	0.26	13.63
K <sub>2</sub> O	0.93	0.87	0.65	2.53	1.43	0.02
H <sub>2</sub> O	-	18.25	-	-	21.99	-
<b>Total</b>	87.40	99.98	87.75	83.31	98.92	89.26

Oxygen basis						
	72	72	72	24	24	10
Cation numbers						
Si	26.811	26.883	26.799	8.430	8.642	3.027
Ti	-	-	0.004	-	-	-
Al	9.182	9.172	9.290	3.471	3.376	1.994
Mg	-	0.092	0.002	0.011	0.044	-
Fe <sup>2+</sup>	-	0.126	0.009	0.001	0.034	0.003
Mn	0.001	-	0.003	-	-	-
<b>Sum</b>	<b>35.994</b>	<b>36.273</b>	<b>36.107</b>	<b>11.913</b>	<b>12.096</b>	<b>5.024</b>
Ca	4.141	3.589	4.135	1.434	1.207	0.107
Sr	0.017	0.008	-	0.194	0.150	0.001
Ba	-	-	0.003	-	-	-
Na	0.362	0.666	0.245	0.066	0.087	1.686
K	0.532	0.530	0.371	0.522	0.314	0.001
<b>Sum</b>	<b>5.052</b>	<b>4.793</b>	<b>4.754</b>	<b>2.216</b>	<b>1.758</b>	<b>1.795</b>
H	-	58.086	-	-	25.268	-

\*: Wet chemical analyses.

**Table 2.** Continued  
b. Stilbite and natrolite-bearing fractures.

#### 4.5. Prehnite

Prehnite occurs as radiated fibrous aggregates of white to brownish tabular crystals up to 0.5 mm long, associated with laumontite. The crystals show a pearly luster and a perfect {001} cleavage. The unit-cell parameters refinement results in  $a = 4.623(1)$ ,  $b = 5.484(2)$ , and  $c = 18.47(2)$  Å. The microprobe analysis (Table 2a, column 2) are in very good agreement with the ideal formula, Ca<sub>2</sub>Al<sub>2</sub>Si<sub>3</sub>O<sub>10</sub>(OH)<sub>2</sub> (Mandarino, 1999).

#### 4.6. Pumpellyite-(Fe<sup>2+</sup>)

In the fractures crosscutting the rocks from Bertrix, pumpellyite forms radiated fibrous aggregates of emerald green to blue acicular crystals. The aggregates, up to 5 mm diameter, are associated with calcite, K-feldspar, and with a green mineral giving a X-ray powder diffraction pattern similar to that of chlorite (Fig. 2).

The structural formula derived from electron microprobe analyses (Table 2d, columns 1 and 2) was calculated according to the single-crystal structure refinement of pumpellyite performed by Yoshiasa & Matsumoto (1985), and corresponds to (Ca<sub>1.99</sub>Na<sub>0.01</sub>)<sub>Σ2.00</sub>(Al<sub>0.42</sub>Fe<sup>2+</sup><sub>0.34</sub>Mg<sub>0.24</sub>Mn<sub>0.01</sub>)<sub>Σ1.01</sub>Al<sub>2.00</sub>(SiO<sub>4</sub>)(Si<sub>2</sub>O<sub>7</sub>)(OH)<sub>2</sub>·H<sub>2</sub>O. The M(1) site is filled with Al, whereas the M(2) crystallographic site contains 0.41-0.43 Al, 0.34 Fe<sup>2+</sup>, and 0.23-0.24 Mg. Consequently, the mineral from Bertrix must be considered as Al-rich pumpellyite-(Fe<sup>2+</sup>), because Fe<sup>2+</sup> > Mg on the M(2) site. Of course, there is really no evidence for these site occupancies just from the chemical analyses.

The unit-cell parameters of pumpellyite from Bertrix correspond to  $a = 8.818(2)$ ,  $b = 5.898(2)$ ,  $c = 19.126(6)$  Å, and  $\beta = 97.26(3)^\circ$ , and are in very good agreement with the parameters published by Yoshiasa & Matsumoto (1985) for an Al-rich pumpellyite sample.

#### 4.7. Other minerals

The microprobe analyses of the minerals occurring in the fractures, and also of those occurring in the country rocks, are reported in Table 2. Several comments can be made on these minerals. Calcite has been observed in the pumpellyite-bearing fractures (Figs 1 and 2), and the microprobe analyses (Table 2d, column 3, 4, and 5) indicate two different compositions, a Mn-rich one (2.60-2.63 % MnO) and a Mn-poor one (0.65 % MnO). Calcite with a Mn-poor composition also occurs in the country rocks of pumpellyite-bearing fractures (Table 2e). The microprobe analyses of chlorite, which occurs in the laumontite-bearing fractures and in the country rock of stilbite-bearing and pumpellyite-bearing fractures (Tables 2a, 2c and 2e), show compositions corresponding to those of chamosite, with Fe<sup>2+</sup> > Mg. Plagioclase occurs in the country rocks, and the microprobe analyses indicate two different compositions, a Ca-poor one with an anorthite content of ~ 5 % (Table 2e, columns 3 and 5), and a

Ca-rich one with an anorthite content of ~ 25 to 30 % (Table 2c, column 2 and Table 2e, column 4). Finally, it is interesting to note that ilmenite shows a significant Mn-content, up to 5.19 % MnO (Table 2c, column 5 and Table 2e, column 9).

## 5. Genetic considerations

As demonstrated by Antun (1953) and more recently by Hatert (1998), the crystallisation of zeolite minerals in the fractures crosscutting the rocks from the Libramont-Bertrix area provides important indications concerning the P-T conditions occurring during the retrograde metamorphic evolution. Whereas the host rock is affected by a lower amphibolite facies metamorphism (Theye & Fransolet, 1993), the minerals occurring in the fractures indicate low-grade conditions.

The P-T stability fields of the minerals plagioclase, stilbite, heulandite, lawsonite, and wairakite, calculated with the thermodynamic data set of Holland & Powell (1998), are shown in Fig. 10. For plagioclase, the anorthite content is fixed to 5 % as measured in the host rock of the pumpellyite-bearing samples (Table 2e, columns 3 and 5). The plagioclase with an anorthite content of ~ 25 to 30 (Table 2c, column 2 and Table 2e, column 4) has probably crystallised at higher P-T conditions, and the albite-rich plagioclase are more likely to coexist with zeolites in chemical equilibrium. According to these calculations, during cooling from peak metamorphic conditions of 4 kbar/500°C (Theye & Fransolet 1993), laumontite should appear in the range of 250°C, and stilbite between 150°C

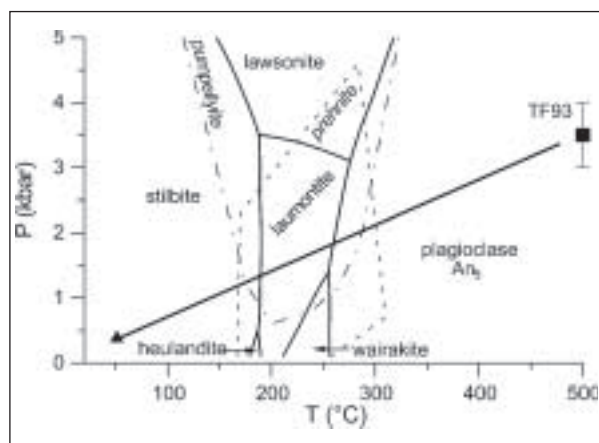


**Figure 10.** P-T diagram with stability fields of the minerals stilbite, heulandite, lawsonite, wairakite, and plagioclase (with anorthite content fixed to 5 %) shown by heavy lines, calculated with thermodynamic data of Holland & Powell (1998). The fields for pumpellyite (dot-dashed) and for prehnite (dashed) are the maximum P-T stabilities as calculated by Frey *et al.* (1991). Peak metamorphic conditions of 3-4 kbar / 500°C are according to Theye & Fransolet (1993). A possible cooling path is indicated by a thick arrow.

wt % :	Ms	Pl	Chl	Bt	Ilm
No. :	Bert6	Bert6	Bert6	Bert6	Bert6
n :	9	3	3	8	2
SiO <sub>2</sub>	46.42	59.79	25.68	35.54	0.76
TiO <sub>2</sub>	0.33	0.01	0.08	1.57	51.21
Al <sub>2</sub> O <sub>3</sub>	33.45	25.49	23.75	19.13	0.05
MgO	1.57	0.04	11.60	9.01	0.01
FeO	3.07	0.24	25.73	20.57	41.94
MnO	0.04	0.03	0.51	0.28	4.80
CaO	0.05	6.82	0.04	0.08	0.02
BaO	0.23	0.01	0.03	0.12	1.57
Na <sub>2</sub> O	0.49	8.00	0.06	0.12	0.02
K <sub>2</sub> O	8.99	0.16	0.68	7.89	0.05
<b>Total</b>	<b>94.64</b>	<b>100.59</b>	<b>88.16</b>	<b>94.31</b>	<b>100.43</b>

Oxygen basis					
	11	8	14	11	3
Cation numbers					
Si	3.118	2.656	2.698	2.726	0.019
Ti	0.016	tr.	0.007	0.091	0.975
Al	2.648	1.335	2.940	1.730	0.001
Mg	0.157	0.002	1.816	1.030	tr.
Fe <sup>2+</sup>	0.172	0.009	2.261	1.320	0.888
Mn	0.002	0.001	0.046	0.018	0.103
<b>Sum</b>	<b>6.113</b>	<b>4.003</b>	<b>9.768</b>	<b>6.915</b>	<b>1.986</b>
Ca	0.004	0.325	0.005	0.006	tr.
Ba	0.006	tr.	0.001	0.004	0.016
Na	0.063	0.689	0.012	0.018	0.001
K	0.770	0.009	0.091	0.772	0.002
<b>Sum</b>	<b>0.843</b>	<b>1.023</b>	<b>0.109</b>	<b>0.800</b>	<b>0.019</b>

**Table 2.** Continued  
c. Country rock of stilbite-bearing fractures.

wt % :	<b>Pmp</b>	<b>Pmp</b>	<b>Cal</b>	<b>Cal</b>	<b>Cal</b>	<b>Kfs</b>	<b>Kfs</b>
No. :	<b>Bert7</b>	<b>Bert9</b>	<b>Bert7</b>	<b>Bert9</b>	<b>Bert9</b>	<b>Bert7</b>	<b>Bert9</b>
n :	<b>5</b>	<b>3</b>	<b>4</b>	<b>5</b>	<b>4</b>	<b>8</b>	<b>10</b>
<b>SiO<sub>2</sub></b>	36.80	37.37	0.22	0.04	0.04	64.51	64.72
<b>TiO<sub>2</sub></b>	0.03	0.02	0.01	0.02	0.02	0.01	0.01
<b>Al<sub>2</sub>O<sub>3</sub></b>	25.11	25.66	0.14	0.02	0.02	18.29	18.18
<b>MgO</b>	1.96	1.96	0.15	0.14	0.05	0.01	0.03
<b>FeO*</b>	4.94	5.01	0.27	0.18	0.13	0.11	0.13
<b>MnO</b>	0.08	0.13	2.60	2.63	0.65	0.03	0.02
<b>CaO</b>	22.88	23.12	62.66	62.12	63.18	0.06	0.05
<b>BaO</b>	0.01	0.01	0.03	0.02	-	0.21	0.16
<b>Na<sub>2</sub>O</b>	0.03	0.04	0.03	0.04	0.03	0.13	0.12
<b>K<sub>2</sub>O</b>	0.01	0.02	0.01	0.05	0.02	16.15	15.79
<b>Total</b>	91.85	93.34	66.12	65.26	64.14	99.51	99.21

<b>Oxygen basis</b>							
	**	**	3	3	3	8	8
<b>Cation numbers</b>							
<b>Si</b>	3.000	2.998	0.003	0.001	0.001	2.999	3.009
<b>Ti</b>	0.002	0.001	tr.	tr.	tr.	tr.	tr.
<b>Al</b>	2.413	2.426	0.002	tr.	tr.	1.002	0.996
<b>Mg</b>	0.238	0.234	0.003	0.003	0.001	0.001	0.002
<b>Fe2+</b>	0.337	0.336	0.003	0.002	0.002	0.004	0.005
<b>Mn</b>	0.006	0.009	0.031	0.032	0.008	0.001	0.001
<b>Sum</b>	5.996	6.004	0.042	0.038	0.012	4.007	4.013
<b>Ca</b>	1.998	1.987	0.952	0.960	0.987	0.003	0.002
<b>Ba</b>	tr.	tr.	tr.	tr.	tr.	0.004	0.003
<b>Na</b>	0.005	0.006	0.001	0.001	0.001	0.012	0.011
<b>K</b>	0.001	0.002	tr.	0.001	tr.	0.958	0.936
<b>Sum</b>	2.004	1.995	0.953	0.962	0.988	0.977	0.952

\* It is not necessary to introduce Fe3+ to obtain charge balance.

\*\* The cation numbers for pumpellyite have been calculated on the basis of 8 atoms per formula unit.

**Table 2.** Continued  
d. Pumpellyite-bearing fractures.

wt % :	Ms	Ms	P1	P1	P1	Kfs	Cal	Chl	Ilm
No. :	Bert7	Bert9	Bert7	Bert7	Bert9	Bert9	Bert7	Bert7	Bert7
n :	13	2	18	10	6	1	1	10	4
SiO <sub>2</sub>	47.15	46.39	67.29	61.86	67.06	64.89	0.19	25.00	0.19
TiO <sub>2</sub>	0.41	0.37	0.03	0.01	0.02	-	0.02	0.11	52.46
Al <sub>2</sub> O <sub>3</sub>	33.54	34.66	20.16	23.54	20.28	17.89	0.01	21.83	0.03
MgO	1.20	0.90	0.04	0.05	0.06	0.01	0.06	13.18	0.05
FeO	1.65	1.44	0.28	0.25	0.26	0.15	0.21	27.19	41.86
MnO	0.03	0.01	0.02	0.02	0.02	0.03	0.27	0.40	5.19
CaO	0.05	0.02	1.18	5.45	0.94	0.02	64.17	0.05	0.04
BaO	0.28	0.30	0.02	0.02	0.02	0.13	-	0.01	-
Na <sub>2</sub> O	0.59	0.65	11.21	8.62	11.09	0.35	0.02	0.02	0.03
K <sub>2</sub> O	10.08	10.23	0.19	0.11	0.44	15.36	0.04	0.09	0.04
<b>Total</b>	94.98	94.97	100.42	99.93	100.19	98.83	64.99	87.88	99.89

Oxygen basis									
	11	11	8	8	8	8	3	14	3
Cation numbers									
Si	3.152	3.103	2.944	2.750	2.942	3.022	0.003	2.660	0.005
Ti	0.020	0.019	0.001	tr.	0.001	-	tr.	0.009	0.991
Al	2.642	2.732	1.039	1.233	1.048	0.982	tr.	2.737	0.001
Mg	0.119	0.089	0.003	0.004	0.004	0.001	0.001	2.089	0.002
Fe <sup>2+</sup>	0.092	0.080	0.010	0.009	0.010	0.006	0.002	2.419	0.879
Mn	0.002	0.001	0.001	0.001	0.001	0.001	0.003	0.036	0.110
<b>Sum</b>	<b>6.027</b>	<b>6.024</b>	<b>3.998</b>	<b>3.997</b>	<b>4.006</b>	<b>4.012</b>	<b>0.009</b>	<b>9.950</b>	<b>1.988</b>
Ca	0.004	0.001	0.055	0.260	0.044	0.001	0.986	0.006	0.001
Ba	0.007	0.008	tr.	tr.	tr.	0.002	tr.	0.001	-
Na	0.077	0.085	0.951	0.743	0.944	0.031	0.001	0.003	0.001
K	0.859	0.873	0.011	0.006	0.024	0.912	0.001	0.012	0.001
<b>Sum</b>	<b>0.947</b>	<b>0.967</b>	<b>1.017</b>	<b>1.009</b>	<b>1.012</b>	<b>0.947</b>	<b>0.988</b>	<b>0.022</b>	<b>0.003</b>

**Table 2.** Continued  
e. Country rock of pumpellyite-bearing fractures.

and 200°C. The very low-pressure minerals heulandite and wairakite do not appear in the Bertrix rocks. A high-pressure limit of 3 - 4 kbar for the formation of the described assemblage is indicated by the absence of lawsonite. The maximum stability ranges of prehnite and pumpellyite (Frey *et al.*, 1991) being associated with observed laumontite assemblage are compatible with the stability field of the latter mineral.

According to these data, laumontite formation at 2 +/- 1 kbar, 200 - 250°C is indicated. This P-T range represents an extensional event and lies on a smooth retrograde cooling path. It is important to note that among all the fracture minerals, only laumontite can provide useful information on the P-T conditions.

According to Fielitz & Mansy (1999), a first metamorphic event M1 is related to a diastathermal metamorphism in a high heat flow extensional regime. The peak metamorphic conditions may be related to this event. Later contractional tectonics leading to nappe stacking was responsible for a second metamorphic imprint M2 under lower-grade P-T conditions. Perhaps extensional tectonics related to the unroofing of the nappe stack is associated to the formation of zeolite bearing extensional veins. The derived P-T conditions would then represent conditions of late stages of the metamorphic event M2.

**Acknowledgements.** Many thanks are due to A.-M. Fransolet and W. Schreyer, for their critical readings of the first version of the manuscript, as well as to P. Antun, M. Blondieau, J. Dehove, M. Houssa & F. Coune, who collected and gave us some samples from Bertrix. The first author acknowledges the F.N.R.S. (Belgium) for a position of "Chargé de Recherches".

## 6. References

- ANTUN, P., 1953. Laumontite de Serpont. *Annales de la Société géologique de Belgique*, 77: B63-B71.
- BEUGNIES, A., 1986. Le métamorphisme de l'aire anticlinale de l'Ardenne. *Hercynia*, II: 17-33.
- BURNHAM, C.W., 1991. LCLSQ version 8.4, least-squares refinement of crystallographic lattice parameters. Dept. of Earth & Planetary Sciences, Harvard University, 24 p.
- CALLIGARIS, M., NARDIN, G., RANDACCIO, L. & CHIARAMONTI, P.C., 1982. Cation-site location in natural chabazite. *Acta Crystallographica*, B38: 602-605.
- CHEN, T.T. & CHAO, G.Y., 1980. Tetranatrolite from Mont St-Hilaire, Québec. *Canadian Mineralogist*, 18: 77-84.
- COOMBS, D.S., ALBERTI, A., ARMBRUSTER, T., ARTIOLI, G., COLELLA, C., GALLI, E., GRICE, J.D., LIEBAU, F., MANDARION, J.A., MINATO, H., NICKEL, E.H., PASSAGLIA, E., PEACOR, D.R., QUARTIERI, S., RINALDI, R., ROSS, M., SHEPPARD, R.A., TILLMANN, E. & VEZZALI, G., 1998. Recommended nomenclature for zeolite minerals: Report of the subcommittee on zeolites of the International Mineralogical Association, Commission on New Minerals and Mineral Names. *European Journal of Mineralogy*, 10: 1037-1081.
- DOWTY, E., 1994. Shape for Windows, version 5.0. A computer program for displaying crystal morphology. Shape Software, Kingsport, TN.
- FIELITZ, W. & MANSY, J.-L., 1999. Pre- and synorogenic burial metamorphism in the Ardenne and neighbouring areas (Rhenohercynian zone, central European Variscides). *Tectonophysics*, 309: 227-256.
- FREY, M., DE CAPITANI, C. & LIOU, J.G., 1991. A new petrogenetic grid for low-grade metabasites. *Journal of Metamorphic Geology*, 9: 497-509.
- GHOBARKAR, H., SCHÄF, O., GUTH, U., 1999. The morphology of hydrothermally synthesized stilbite type zeolites. *Journal of Solid State Chemistry*, 142: 451-454.
- HATERT, F., 1998. Données nouvelles sur la laumontite de la zone métamorphique de Libramont, Belgique. *Geologica Belgica*, 1: 3-7.
- HOLLAND, T.J.B. & POWELL, R., 1998. An internally consistent thermodynamic data set for phases of petrological interest. *Journal of Metamorphic Geology*, 16: 309-343.
- LIBOWITZKY, E., 1999. Correlation of O-H stretching frequencies and O-H...O hydrogen bonds lengths in minerals. *Monatshefte für Chemie*, 130: 1047-1059.
- MANDARINO, J.A., 1999. Fleischer's glossary of mineral species. The Mineralogical Record Inc., Tucson, 225 p.
- PASSAGLIA, E., 1970. The crystal chemistry of chabazites. *American Mineralogist*, 55: 1278-1301.
- PASSAGLIA, E., GALLI, E., LEONI, L. & ROSSI, G., 1978. The crystal chemistry of stilbites and stellerites. *Bulletin de Minéralogie*, 101: 368-375.
- PECHAR, F. & RYKL, D., 1983. Study of the complex vibrational spectra of natural zeolite chabazite. *Zeolites*, 3: 333-336.
- PECHAR, F. & RYKL, D., 1985. Infrared spectra of natural zeolites. Academia Nakladatelství CSAV (Československá Akademie Ved), Praha, 68 p.
- QUARTIERI, S. & VEZZALINI, G., 1987. Crystal chemistry of stilbites: structure refinements of one normal and four chemically anomalous samples. *Zeolites*, 7: 163-170.
- ROSS, M., FLOHR, J.K. & ROSS, D.R., 1992. Crystal-line solution series and order-disorder within the natrolite mineral group. *American Mineralogist*, 77: 685-703.
- THEYE, T. & FRANSOLET, A.M., 1993. Amphibolit-fazielle Metamorphite im Rhenohercynikum der Ardenen. *Berichte der Deutschen Mineralogischen Gesellschaft, Beihefte zur European Journal of Mineralogy*, 5: 255.
- YOSHIASA, A. & MATSUMOTO, T., 1985. Crystal structure refinement and crystal chemistry of pumpellyite. *American Mineralogist*, 70: 1011-1019.

Manuscript received 7.07.2003; accepted for publication 8.03.2004.